

# ACAUSAL MODELING AND SIMULATION OF THE STANDALONE SOLAR POWER SYSTEMS AS HYBRID DAEs

Arash M. Dizqah<sup>\*1</sup>, Krishna Busawon<sup>1</sup> and Peter Fritzson<sup>2</sup>

<sup>1</sup>School of Computing, Engineering and Information Sciences , Northumbria University, NE1 8ST Newcastle Upon Tyne, UK

<sup>2</sup>PELAB Programming Environment Lab, Dep. Computer Science , Linköping University, SE-581 83 Linköping, Sweden

**Abstract**—Due to the presence of algebraic constraints as well as existing of different modes of operation, a standalone solar power system consisting of photovoltaic arrays, battery bank, electrical load, and a converter is becoming a complex system that can no longer be modeled using the conventional block diagram approach. While the block diagram approach is based on causal interactions between a chain of the ordinary differential equations (ODE), a more appropriate acausal approach solves a flat model of the system consisting of hybrid differential algebraic equations (HDAE). In effect, this paper proposes a nonlinear HDAE-based model of a standalone solar power system. The proposed model is presented using the Modelica language that allows object-oriented and acausal modeling of the multi-mode systems. Next, a general purpose solver is employed to simulate the system. The results of the simulation shows proper match with the information available in the components datasheet. It is shown that the simulation provides a sufficiently accurate prediction of all the system behaviors, which is vital for any model-based controller, including mode transitions.

**Index Terms**—hybrid DAE; photovoltaic (PV); battery; boost-type DC-DC converter; Modelica; acausal modeling; standalone solar power.

## I. INTRODUCTION

**A**DVANCES in photovoltaic (PV) technologies during the last decade have increased the share of the solar energy in the growing electricity market. The PV modules are nonlinear and complex still very popular components since they are easy to install and operate. A conventional solar power system employs an array of PV modules as a generator to supply DC, AC, or mixed electrical load demands. It consists of a converter that normally boosts up the generated DC voltage to match the load characteristics. This converter is equipped with a maximum power point tracker (MPPT) to harvest the maximum available power. The system may optionally consist of an inverter for being connected to AC loads or the grid. Moreover, it consists of a battery bank to overcome the power fluctuation that is the result of the uncertainty in the solar irradiance. The battery also provides a constant voltage bus, which is essential for the MPPT algorithm. Although the voltage changes with regard to the amount of the current as

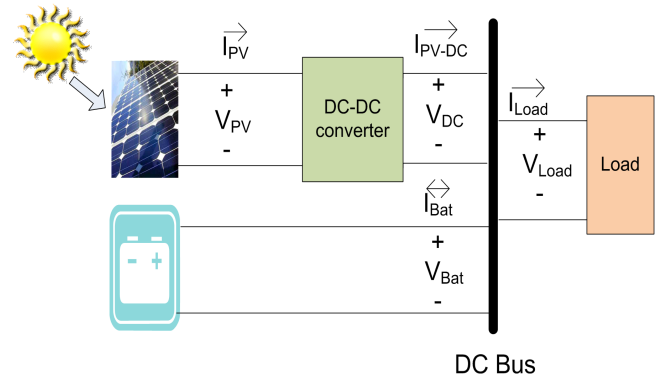


Fig. 1. HRES topology in this study.

well as the state of the charge (SOC) of the battery, it can be assumed constant during the time that the MPPT calculates the operating point. Figure 1 illustrates the topology of the standalone solar power system selected in this study.

In order to study the behavior of the solar power system as well as to design model-based controllers, it is essential to model and simulate the system accurately. However, there are two major challenges, namely, the algebraic constraints introduced by the PV module and the battery, and the multi-mode operation of the battery. Altas and Sharaf [1] used the simplification techniques introduced by Buresch [2] as well as the Simulink basic components to model and simulate the solar power system consisting of a PV module. Since the Simulink basic components, which provide classical block diagram simulation approach, does not support algebraic states, they introduced a weak dynamic as a short transport delay to their model. Villalva, Gazoli and Filho [3] proposed two simulation scenarios based on equivalent electrical circuits, to simulate the PV module. The proposed scenarios in [3] employ the SimPowerSystems that is one of the Simulink toolboxes for acausal simulation to overcome the algebraic loop introduced by the PV module. The acausal simulation needs the system to be modeled as differential algebraic equations (DAE). Petcut and Dragomir [4] introduced a first-order differential equation associated to the original algebraic equation of the PV module.

\*Corresponding author. Email address: arash.moradinegade@northumbria.ac.uk

They proved that the equilibrium point of this differential equation and the solution of the algebraic equation are exactly the same. Introducing this differential equation, they modeled and simulated a PV module with Simulink basic components. Carrero, Amador, and Arnaltes [5] simply fed back the output current of the PV module that introduces algebraic loop. Guasch and Silvestre [6] proposed a comprehensive model for lead-acid batteries along with an equivalent electrical circuit appropriate for simulation. However, their model needs an acausal approach to be simulated because of proposed algebraic loops. Moreover, they introduced a linear interpolation to simulate the mode transition period without considering it as a multi-mode (or in general hybrid) system. Tremblay and Dessaint [7] employed the Simulink SimPowerSystems toolbox to propose an acausal simulation of the lead-acid battery.

Due to the presence of algebraic constraints, the standalone solar power system cannot be decomposed into a chain of blocks with causal interaction and it requires being simulated employing an acausal approach [8]. Moreover, the different modes of operation introduced by battery cause discontinuity points in overall system mathematical model and classify it as an hybrid system [9]. In this paper, a mathematical model of the standalone solar power system is proposed as HDAEs. The Modelica is employed to create an acausal model of the system and the developed model is solved using a general purpose solver. The results of the simulation have been compared with information available in the PV and the battery datasheets provided by the manufacturers that indicate good accuracy.

An outline of the paper is as follows: In the next section, the mathematical models of the system components are presented. Section 3 provides the employed simulation method as well as an overview of the developed Modelica model. The results and their validations are discussed in Section 4. Finally, Section 5 presents a conclusion of the study.

## II. SOLAR POWER SYSTEM MATHEMATICAL MODEL

### A. PV module and PV array

A PV cell is a P-N junction that is typically modeled with an equivalent electrical circuit [10]. Fig. 2 illustrates a single-diode equivalent electrical circuit of a PV cell, which is also applicable to model a PV module. The PV module consists of several PV cells connected together in series. A PV array, which is a combination of several photovoltaic modules in series and parallel arrangement, can be modeled with the same circuit, too. There are six electrical parameters in this model, namely, the stray capacity  $C$  that can be neglected, the ideality factor of the diode  $n_D$ , the photocurrent  $I_{ph}$ , the reverse saturation current of the diode  $I_0$ , the series resistor  $R_s$ , and the shunt resistor  $R_{sh}$ . While the series resistor  $R_s$  is the sum of structural resistances, the shunt resistor  $R_{sh}$  represents the leakage current [11]. There are prior researches to estimate the electrical parameters from the PV module information available in datasheet [3], [11], [12]. Through this study, it is assumed that the equivalent electrical circuit of the PV module has already been identified using one of these methods. In Fig.

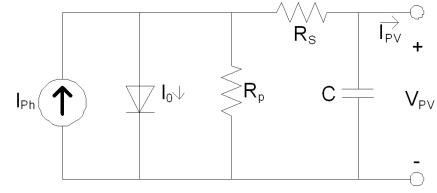


Fig. 2. The single-diode equivalent electrical circuit of a PV module.

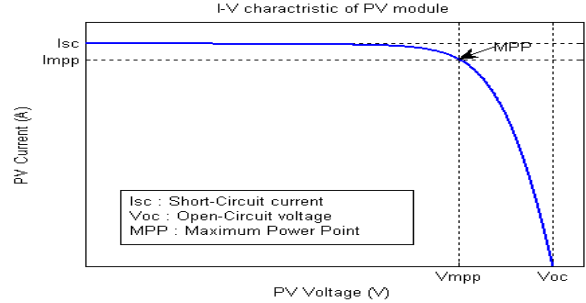


Fig. 3. The  $I - V$  curve of the PV module for the STC.

2, applying the Kirchhoff current law (KCL) to the junction point of these two resistors gives the characteristic equation of the PV module, which is a nonlinear transcendental equation, as follows:

$$I_{pv} = I_{ph} - I_0 \left\{ \exp\left(\frac{V_{pv} + R_s I_{pv}}{n_d N_s} \frac{q}{KT_c}\right) - 1 \right\} - \frac{V_{pv} + R_s I_{pv}}{R_{sh}} \quad (1)$$

where  $V_{pv}$  and  $I_{pv}$  are, respectively, the output voltage and current of the PV module and all other symbols are defined as follows:

$q$	The electron charge ( $1.6021810^{-19}$ )
$K$	The Boltzman constant ( $1.3806610^{-23}$ )
$N_s$	The number of the PV cells in series as the PV module (-)
$T_c$	The current amount of the PV cell temperature ( $K$ )

The photocurrent  $I_{ph}$  and the reverse saturation current of the diode  $I_0$  are calculated with (2) and (3) based on available parameters in the datasheets and the estimated electrical parameters [3], [13]. The performance of different PV modules are measured at a standard test condition (STC), which is defined as follows:

- The cell temperature of  $25C$
- The Global solar irradiance of  $1000(W/m^2)$
- Air Mass of 1.5

Fig. 3 shows the PV current-voltage ( $I - V$ ) curve indicating the maximum power point (MPP). The MPP varies due to changes in operating conditions (i.e. the solar irradiance and the cell temperature) and requires being followed by a MPPT algorithm.

$$I_{ph} = \left( \frac{R_s + R_{sh}}{R_{sh}} I_{sc, stc} + k_I (T_c - T_{c, stc}) \right) \frac{S}{S_{stc}} \quad (2)$$

$$I_0 = \frac{I_{sc, stc} + k_I (T_c - T_{c, stc})}{\exp\left(\frac{V_{oc, stc} + k_V (T_c - T_{c, stc})}{n_d N_s} \frac{q}{K T_c}\right) - 1}. \quad (3)$$

where:

$I_{sc, stc}$	The short-circuit current of the PV module at the STC (A)
$k_I$	The temperature coefficient of the short-circuit current (A/C)
$k_V$	The temperature coefficient of the open-circuit voltage (V/C)
$S$	The current amount of the solar irradiance (W/m)
$S_{stc}$	The amount of the solar irradiance for the STC (W/m)
$T_{c, stc}$	The amount of the cell temperature at the STC (K)
$V_{oc, stc}$	The open-circuit voltage of the PV module at the STC (V)

The PV array of the solar power system introduces an algebraic nonlinear constraints between  $V_{PV}$  and  $I_{PV}$ , i.e., none of these variables are among degrees of freedom and the former is an algebraic state.

### B. Boost-Type DC-DC converter

The boost-type DC-DC converter is one of the converter options which is implemented based on the switching-mode circuit technology containing at least one energy storage and two semiconductor switches. However, in the ideal case a single-pole double-throw switch can be used. Figure 4 illustrates the electrical circuit for a boost-type DC-DC converter with an ideal switch.

Middlebrook and Cuk [14] proposed a state-space averaging approach to model the boost-type DC-DC converter. They suggested two  $i_L$  and  $v_C$  states for the continuous conduction mode (CCM) in which the instantaneous inductor current is always greater than zero. According to the proposed approach there is a state-space system for the converter at each state of the switch and the overall state-space model is the weighted average of these two models. The weighting factor is switching duty-cycle ( $D$ ) as the only manipulating control signal. The switching duty-cycle is the duration of time that the circuit remains in each state. Equations (4) and (5) provide the average model of the boost-type DC-DC converter using ideal switch and diode.

$$\begin{bmatrix} \dot{i}_L(t) \\ \dot{v}_C(t) \end{bmatrix} = \begin{bmatrix} -\frac{R_L}{L} - \frac{R_C(1-D)}{L(1+\frac{R_C}{R})} & -\frac{1-D}{L(1+\frac{R_C}{R})} \\ \frac{1-D}{C(1+\frac{R_C}{R})} & -\frac{1}{RC(1+\frac{R_C}{R})} \end{bmatrix} \times \quad (4)$$

$$\begin{bmatrix} i_L(t) \\ v_C(t) \end{bmatrix} + \begin{bmatrix} \frac{1}{L} \\ 0 \end{bmatrix} V_{in}(t). \quad (5)$$

$$V_{out}(t) = \begin{bmatrix} \frac{R_C(1-D)}{1+\frac{R_C}{R}} & \frac{1}{1+\frac{R_C}{R}} \end{bmatrix} \begin{bmatrix} i_L(t) \\ v_C(t) \end{bmatrix}.$$

### C. Lead-acid battery

There are different types of batteries applicable for backup/storage of the solar power system. The authors in [15] [16] presented a comprehensive reviews and comparisons of different battery technologies for the renewable energy applications. The battery introduces an algebraic constraint between

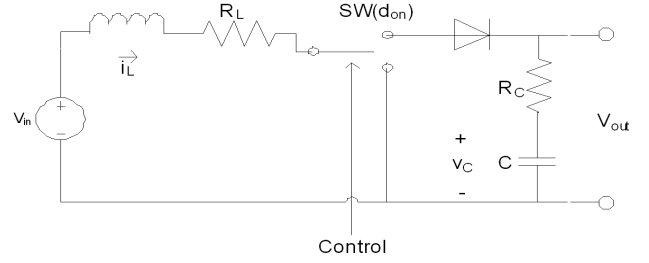


Fig. 4. The electrical circuit of the boost-type DC-DC converter with an ideal switch.

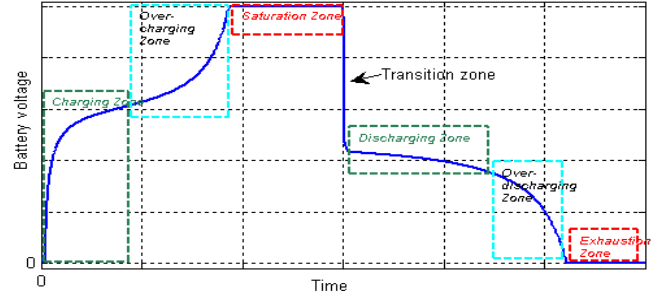


Fig. 5. Different working zones of the lead-acid batteries.

$V_{bat}$  and  $I_{bat}$  where the former is an algebraic state. Fig. 5 illustrates a complete operating cycle of the battery starting from the charging zone up to completely being discharged, i.e., the exhaustion zone [6]. In Fig. 5, it can be seen that the battery is a multi-mode component introducing discontinuity to the system. Tremblay and Dessaint [7] proposed an equivalent electrical circuit (Fig. 6) as well as the following hybrid mathematical presenting two modes of operation, namely, charging, and discharging:

$$V_{bat} = \begin{cases} V_0 - RI_{bat} + V_{exp} - \frac{P_1 C_{max}}{C_{max} - charge} charge - \frac{P_1 C_{max}}{charge + 0.1 C_{max}} I_{bat} & \text{mode=charging,} \\ V_0 - RI_{bat} + V_{exp} + \frac{P_1 C_{max}}{charge - C_{max}} charge + \frac{P_1 C_{max}}{charge - C_{max}} I_{bat} & \text{mode=discharging.} \end{cases} \quad (6)$$

$$mode = \begin{cases} charging & I_{bat} \leq 0, \\ discharging & I_{bat} > 0. \end{cases} \quad (7)$$

$$\frac{dcharge}{dt}(t) = \frac{1}{3600} I_{bat}(t). \quad (8)$$

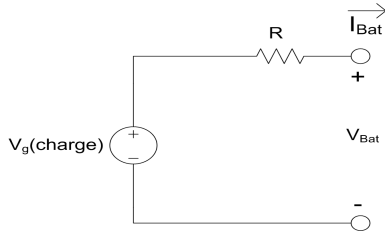


Fig. 6. The equivalent electrical circuit for the lead-acid battery.

$$\frac{dV_{exp}(t)}{dt} = \begin{cases} \frac{P_2}{3600}|I_{bat}|(P_3 - V_{exp}) & \text{mode=charging,} \\ -\frac{P_2}{3600}|I_{bat}|V_{exp} & \text{mode=discharging.} \end{cases} \quad (9)$$

where  $V_{bat}$  and  $I_{bat}$  are the voltage and the current of the battery, respectively. The parameters  $P_1$ - $P_3$  are the experimental parameters requires being identified for each type of the battery and  $V_{exp}$  (V) models the exponential behavior of the battery voltage during the mode transition period. While the current direction varies instantaneously, the voltage of the battery changes with an exponential factor after the mode transition. The  $C_{max}$  is the maximum amount of the battery capacity (Ah),  $R$  is the internal resistor of the battery ( $\Omega$ ),  $charge$  (Ah) is the actual battery capacity, and  $V_0$  is the battery constant voltage (V).

### III. SIMULATION

According to the block diagram approach for modeling and simulation, the system is decomposed into distinguished blocks with causal interactions. In a sequential procedure starting from the first block through all others, the simulator calculates output values with respect to the inputs and then feeds the outputs to the next block as their input variables. Although it is a straightforward approach, it still suffers from several drawbacks. In order to decompose a system into a chain of causal interacting blocks, the system must have just the differential states coupled with algebraic equations to calculate the outputs. In other words, it must be a system of ordinary differential equations (ODE) and any algebraic equation has to calculate only an algebraic variable that is a degree of freedom. However, most of the electrical and mechanical systems introduce algebraic states. An algebraic state is a state of the system which is restricted with an algebraic equation. Any system consisting of algebraic states, which are modeled with DAEs rather than ODEs, requires being simulated employing an acausal approach.

Despite a causal model which expresses an algorithm to calculate the variables, the acausal modeling is a declarative approach in which individual parts of the model are directly described as equations that are in general HDAEs. An HDAE represents both continuous-time (either differential or algebraic) and discrete-time behaviors [9]. Although there are general purpose numerical HDAE solvers such as tools in [17],[18],[19], the acausal modeling still needs to be described with a programming language. Modelica [20], which is an object-oriented and equation-based language providing the

TABLE I  
THE FIRST PLANE OF THE MODELICA CODES MODELING THE SOLAR POWER SYSTEM.

#### model HRES\_SolarSystem

```

Modelica.Blocks.Sources.Constant Sx(k = 300.0);
Modelica.Blocks.Sources.Constant Tx(k = 298.15);
Modelica.Electrical.Analog.Basic.Ground ground;
HRES.PVArray pvarray(Npvp = 10);
Modelica.Blocks.Sources.TimeTable DutyCycle(table = [...]);
Modelica.Blocks.Sources.Step ramp(startTime = 5, offset = 10,
height = -6);
Modelica.Electrical.Analog.Basic.VariableResistor load;
HRES.BoostConverter converter(RI = 0.001, Rc = 0.3, L = 0.0005,
C = 0.005);
HRES.LeadAcidBattery battery1;
HRES.LeadAcidBattery battery2;
HRES.LeadAcidBattery battery3;
HRES.LeadAcidBattery battery4;

```

#### equation

```

connect(Tx.y,pvarray.Tx);
connect(Sx.y,pvarray.Sx);
connect(pvarray.n,ground.p);
connect(pvarray.p,converter.p1);
connect(converter.n1,ground.p);
connect(converter.n2,ground.p);
connect(DutyCycle.y,converter.D);
connect(converter.p2,load.p);
connect(ramp.y,load.R);
connect(load.n,ground.p);
connect(converter.p2,battery1.p);
connect(battery1.n,battery2.p);
connect(battery2.n,battery3.p);
connect(battery3.n,battery4.p);
connect(battery4.n,ground.p);

```

#### end HRES\_SolarSystem;

capability to model the hybrid systems [21], is an option to describe complex systems using an acausal approach. Among a number of available implementations of the Modelica compiler, the OpenModelica platform [22] has been selected for this study chiefly because it supports more features of the Modelica language comparing with the others. The platform translates the Modelica descriptions into a flat model in the form of HDAEs, then generates C or XML code from the flat model. The compiled model is simulated using the integrated DASSL that is a general purpose HDAE solver [19].

Table I shows the first plane of the developed Modelica codes that models the standalone solar power system. From Table I, it can be seen that the proposed model consists of a PV array connected to a resistive load through a converter. A battery bank including four lead-acid batteries is employed to prevent power fluctuations. All these components are also modeled as separate classes of the Modelica language. For instance, Table II summaries such a model for the lead-acid battery and its multi-mode operation.

TABLE II  
A SUMMARY OF THE LEAD-ACID BATTERY MODELICA CLASS.

```

class LeadAcidBattery
...
equation
chargeState = if noEvent(ibat ≤ 0) then true else false;
der(charge) = 1/3600 * ibat;
der(Vexp) = if chargeState then
    P2/3600 * abs(i) * (P3 - Vexp)
else -(P2 * abs(i))/3600 * Vexp;
when change(chargeState) and pre(chargeState) then
    tmp = if not chargeState then
        pre(vbat) - V0 - R * pre(ibat) -
        (P6 * Cmax)/(Cmax - pre(charge)) * pre(charge) -
        (P6 * Cmax)/(pre(charge) + 0.1 * Cmax) * pre(ibat)
    else 0;
    reinit(Vexp, tmp);
end when;
soc = 1 - charge/Cmax;
vbat = if chargeState then
    V0 - R * ibat - (P1 * Cmax)/(Cmax - charge) * charge -
    (P1 * Cmax)/(charge + 0.1 * Cmax) * ibat + Vexp
else V0 - R * ibat - (P1 * Cmax)/(Cmax - charge) * charge -
    (P1 * Cmax)/(Cmax - charge) * ibat + Vexp;
end LeadAcidBattery;

```

#### IV. RESULTS, VALIDATION, AND DISCUSSION

The proposed model is used to simulate a solar power system consisting of an array of the Kyocera KC200GT PV modules [23] and a bank of the Panasonic LC-R127R2PG lead-acid batteries [24]. The authors in [3] and [7], respectively, presented the identified electrical parameters of the PV module and the lead-acid battery that are used in this study.

Fig. 7 shows the simulated current-voltage ( $I - V$ ) and power-voltage ( $P - V$ ) curves of the KC200GT PV module at the STC condition. It is observed that the proposed model predicts the curve very close to the empirical data provided by the manufacturer (the circle markers). The simulated MPP is in the same position of the experimental point as well.

Fig. 8 illustrates the simulation results of the LC-R127R2PG lead-acid battery [24] for a full cycle as in Fig. 5 that is a cycle of charging, over-charging, saturation, discharging, over-discharging, and exhaustion zones. While the battery is being charged for 100 minutes, it is discharged afterward. It also indicates that after 25 minutes it enters into the over-charging zone. Discharging with the current of 7.2A in average, it takes around 35 minutes for the battery, which matches with the information available in datasheet [24], to reach the cut-off voltage that is around 10.2V.

The solar power system is simulated using the proposed model for the following scenario:

- Simulation duration is 10 minutes.
- The solar irradiance is  $1000W/m^2$  and the cell temperature is  $25^\circ C$ .
- The PV array consists of 10 connected KC200GT PV

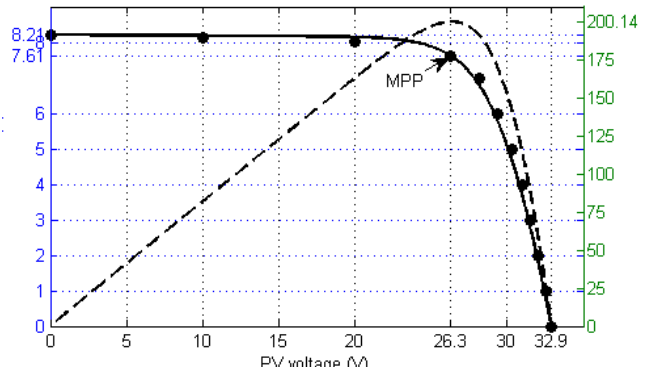


Fig. 7. The simulated current-voltage curve of the KC200GT PV module at the STC.

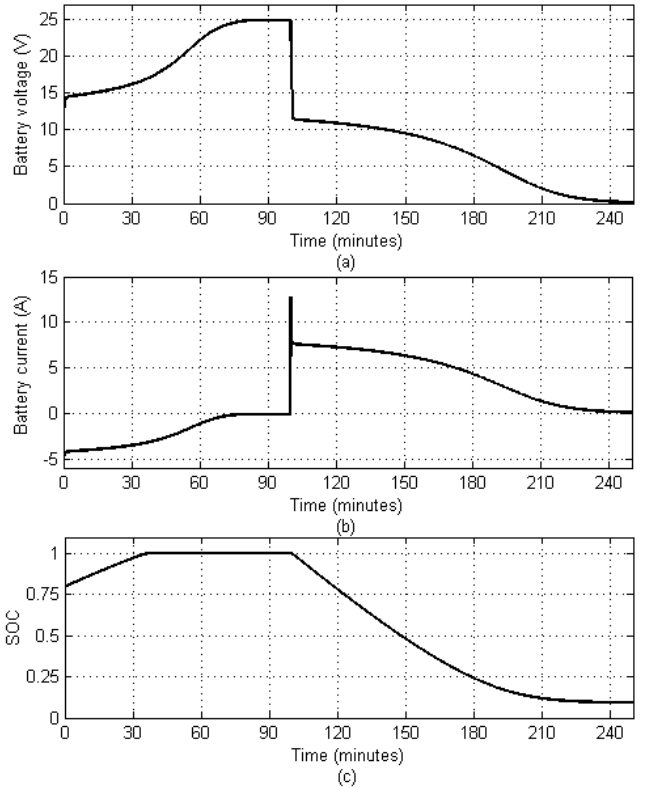


Fig. 8. The simulated (a) battery voltage, (b) battery current, and (c) the SOC of the battery.

modules in parallel arrangement.

- The battery bank consists of 4 connected LC-R127R2PG lead-acid batteries in series arrangement.
- The manipulating control signal changes according to a stepwise pattern.
- The load demand suddenly increases at  $t = 5$ .
- After 6 minutes the generated power by the PV array declines.

In Fig. 9, it can be seen that the battery absorbs excess energy when there is and provides the deficit energy when the PV module cannot provide adequate energy. For the first 5 minutes, the generated power is more than load demand and the battery, which absorbs the excess energy, is in charging mode. The load demand suddenly increases to more than the

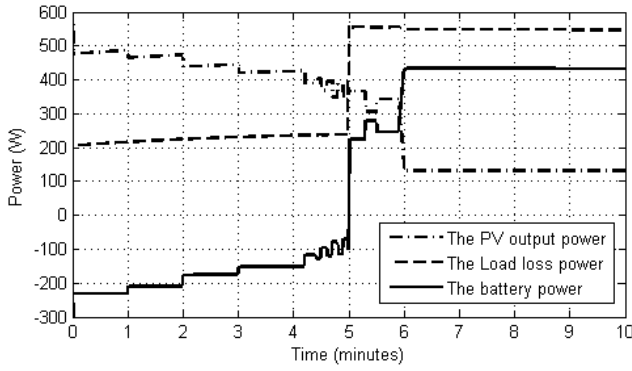


Fig. 9. The simulated battery, load, and PV powers.

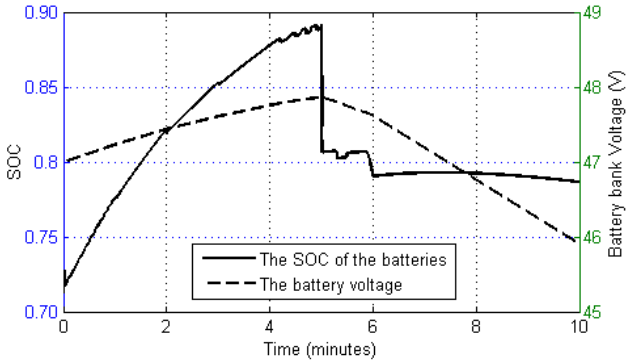


Fig. 10. The simulated SOC and the voltage of battery bank.

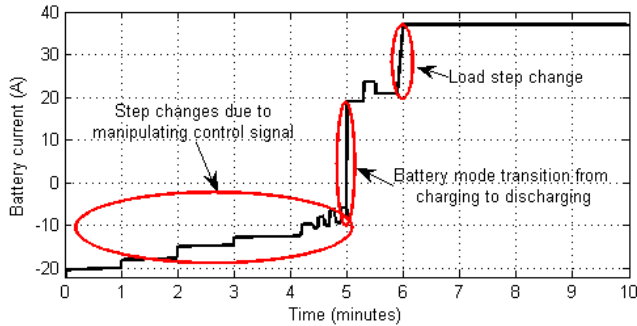


Fig. 11. The simulated battery current.

generated power at  $t = 5$  minutes that switches the state of the battery, which now provides the deficit energy, to the discharging mode. At  $t = 6$  minutes the battery provides more power because the generated power by the PV array declines even less due to manipulating of the control signal. Fig. 9 illustrates a power loss of around 10% in the DC-DC converter, which is the difference of the power generated by the PV array and the sum of the load and the battery powers, chiefly because of the internal resistance of the coil.

Fig. 10 illustrates the details of battery bank. It is observed that during the period of charging of the battery bank ( $time < 5$  minutes), the voltage and the SOC of the battery bank increase continuously. However, the voltage of the battery suddenly falls at  $t = 5$  minutes to the nominal value by the

transition from charging mode to discharging mode. There is another step change at  $t = 6$  minutes as the result of decreasing the generated power by the PV array (Fig. 9). The SOC also declines moderately after  $t = 5$  minutes since the battery is being discharged.

Finally, Fig. 11 depicts the variation of the battery bank current during the simulation period. While it is less than zero, which means the battery bank is in charging mode, before the  $time = 5$  minutes, it suddenly becomes greater than zero after entering in the discharging mode. The small step changes are due to variation in the control signal causing changes in the harvested energy from the PV array. A load demand increase at  $t = 6$  minutes causes a sharp climb of the battery bank current that matches the power variation in Fig. 9.

## V. CONCLUSION

This paper proposes an acausal model, which is based on the HDAE, to simulate the solar power system. The proposed model presents the nonlinear algebraic constraints, which are introduced by the PV array and the battery, as DAEs. Moreover, it models different modes of the battery operation as a hybrid system. The Modelica language is employed to describe the system as an acausal model organized as separate Modelica classes for different components. The OpenModelica environment as an integrated modeling and simulation Modelica tool-set is used to simulate the system with the DASSL general purpose integrator. The PV array and the lead-acid battery bank are separately simulated and validated with information available in datasheets that show very good accuracy. The whole solar power system is also simulated and discussed thoroughly indicating accurate prediction of all the system behaviors including mode transitions. The highest level Modelica codes as well as a summary of the battery Modelica class are presented.

## VI. ACKNOWLEDGMENT

The authors would like to thank the Synchron Technology Ltd. company for their partial financial support of this research.

## REFERENCES

- [1] I. H. Altas, and A. M. Sharaf. A photovoltaic array simulation model for matlab-simulink GUI environment. In *Proc. Intl. Conf. Clean Elect. Power (ICCEP)*, pages 341–345, 2007.
- [2] M. Buresch. *Photovoltaic Energy Systems Design and Installation*. McGraw-Hill, New York, 1983.
- [3] M. G. Villalva, J. R. Gazoli, and E. R. Filho. Comprehensive approach to modeling and simulation of photovoltaic arrays. *IEEE Transactions on Power Electronics*, 24:1198–1208, 2009.
- [4] F. M. Petcut, and T. L. Dragomir. Solar cell parameter identification using genetic algorithms. *Journal of Control Engineering and Applied Informatics*, 12:30–37, 2010.
- [5] C. Carrero, J. Amador, and S. Arnaltes. A single procedure for helping PV designers to select silicon PV

- modules and evaluate the loss resistances. *Journal of Renewable Energy*, 32:2579–2589, 2007.
- [6] D. Guasch, and S. Silvestre. Dynamic battery model for photovoltaic applications. *Progress in Photovoltaics: Research and Applications*, 11:193–206, 2003.
- [7] O. Tremblay, and L. Dessaint. Experimental validation of a battery dynamic model for ev applications. *World Electric Vehicle Journal*, 3:10–15, 2009.
- [8] M. Najafi, and R. Nikoukhah. Modeling and simulation of differential equations in scicos. In The Modelica Association, editor, *Modelica Conference*, 2006.
- [9] H. Lundvall, P. Fritzson, and B. Bachmann. Event handling in the openmodelica compiler and runtime system. In *the 46th Conference on Simulation and Modeling (SIMS 2005)*, Trondheim, Norway, 2005.
- [10] M. K. Deshmukh, and S. S. Deshmukh. Modelling of hybrid renewable energy system. *Renewable And Sustainable Energy Reviews*, 12:235–249, 2008.
- [11] J. J. Soon, and K. S. Low. Photovoltaic model identification using particle swarm optimization with inverse barrier constraints. *IEEE Transactions on Power Electronics*, 27:3975–3983, 2012.
- [12] K. Ishaque, Z. Salam, and H. Taheri. Simple, fast and accurate two-diode model for photovoltaic modules. *Journal of Solar Energy Materials and Solar Cells*, 95:586–594, 2011.
- [13] Q. Kou, S. A. Klein, and W. A. Beckman. A method for estimating the long-term performance of direct-coupled PV pumping systems. *Journal of Solar Energy*, 64:33–40, 1998.
- [14] R. D. Middledbrook, and S. Cuk. A general unified approach to modelling switching-converter power stages. In *Proc. of IEEE Power Electronics Specialist conference*, 1976.
- [15] M. Beaudin, H. Zareipour, A. Schellenbergglabe, and W. Rosehart. Energy storage for mitigating the variability of renewable electricity sources: An updated review. *Energy for Sustainable Development*, 14:302–314, 2010.
- [16] K. C. Divya, and J. Ostergaard. Battery energy storage technology for power systems an overview. *Electric Power Systems Research*, 79:511–520, 2009.
- [17] SUNDIALS. Suite of nonlinear and differential/algebraic equation solver. <https://computation.llnl.gov/casc/sundials/>.
- [18] DAETS. Defferential-algebraic equations by taylor series. [www.cas.mcmaster.ca/ nedialk/dates/](http://www.cas.mcmaster.ca/ nedialk/dates/).
- [19] DASSL. Defferential algebraic system solver. [www.cs.ucsb.edu/~cse/](http://www.cs.ucsb.edu/~cse/).
- [20] Modelica. Modelica association. [www.modelica.org](http://www.modelica.org).
- [21] P. Fritzson. *Introduction to modelling and Simulation of Technical and Physical Systems with Modelica*. John Wiley & Sons, New York, 2011.
- [22] OpenModelica. Open-source modelica-based modeling and simulation env. [www.openmodelica.org](http://www.openmodelica.org).
- [23] Kyocera. KC200GT, high efficiency multicrystal photovoltaic module. [www.kyocerasolar.com/assets/001/5195.pdf](http://www.kyocerasolar.com/assets/001/5195.pdf), 2012.
- [24] Panasonic. LC-R127R2PG, panasonic batteries. [www.farnell.com/datasheets/1624915.pdf](http://www.farnell.com/datasheets/1624915.pdf).